NEUROLOGICAL DISORDERS

Microstructure of the Midbrain and Cervical Spinal Cord in Idiopathic Restless Legs Syndrome: A Diffusion Tensor Imaging Study

Klaas Lindemann, MD[1,*]; Hans-Peter Müller, PhD[1,*]; Albert C. Ludolph, MD[1]; Magdolna Hornyak, MD[1,2,†]; Jan Kassubek, MD[1,†]

*[1]Department of Neurology, University of Ulm, Ulm, Germany; [2]Neuropsychiatrisches Zentrum Erding/München, Erding, Germany; *co-first authors; †co-senior authors*

Study Objectives: Diffusion tensor imaging (DTI) allows the study of white matter microstructure in the central nervous system. The aim of this study was to examine the DTI metrics of the cervical spinal cord and the brainstem up to the midbrain in patients with idiopathic restless legs (RLS) compared to matched healthy controls.

Methods: DTI analysis of the cervical spinal cord and the brainstem up into the midbrain was performed in 25 patients with idiopathic RLS and 25 matched healthy controls. Data analysis in the brain was performed by voxelwise comparison of fractional anisotropy (FA) maps at group level. Cervical spinal cord data analysis was performed by slicewise analysis of averaged FA values in axial slices along the spinal cord.

Results: Voxelwise comparison of FA maps in the brainstem showed significant microstructural alterations in two clusters in the midbrain bilaterally. Slicewise comparison of the FA maps in the cervical spinal cord showed a trend for lower FA values at the level of the second and third vertebra area in the patient sample.

Conclusions: The imaging data suggest that significant alterations in the midbrain in RLS can be visualized by DTI and might correlate to a macroscopically subtle process with changes of the tissue microstructure in the corresponding tracts. An additional area of interest is regionally clustered in the upper cervical spinal cord with a tendency toward altered diffusion metrics. These results might be addressed by further studies, e.g., at higher magnetic field strengths.

Keywords: diffusion tensor imaging, midbrain, restless legs syndrome, spinal cord, magnetic resonance imaging, substantia nigra

Citation: Lindemann K, Müller HP, Ludolph AC, Hornyak M, Kassubek J. Microstructure of the midbrain and cervical spinal cord in idiopathic restless legs syndrome: a diffusion tensor imaging study. *SLEEP* 2016;39(2):423–428.

Significance

Diffusion tensor imaging demonstrated microstructural alterations in the midbrain and in the upper cervical spinal cord in patients with idiopathic restless legs (RLS). These alterations might correlate to a macroscopically subtle process with changes of the tissue microstructure in the corresponding tracts. It is the first time that an unbiased computerized magnetic resonance imaging analysis at the group level unravelled these structures to be altered in structural connectivity in association with RLS. Although many elements are still ill-defined, these results substantially add to the definition of the RLS pathoanatomy as accessible in vivo.

INTRODUCTION

Idiopathic restless legs syndrome (RLS) is a common sensorimotor disorder with a prevalence of 6–12% in Western countries.[1] It is characterized by strong unpleasant sensations, a nearly irresistible urge to move the legs in the evening or at night, and temporary and partial relief of symptoms can be achieved by moving the legs or walking.[2] The pathophysiology and pathoanatomy of the disorder is still not well defined, although different concepts exist including the involvement of the so-called A11 cell group.[3] A11 cells are the only cells that provide dopaminergic axons to the spinal cord; they are clustered in the midbrain close to the hypothalamus and project into the cortex, the limbic system, and the spinal cord.[3,4]

In order to identify morphological correlates of the pathophysiology in the central nervous system *in vivo*, early magnetic resonance imaging (MRI) studies exhibited local decreases of iron in the putamen and the substantia nigra[5]—a finding replicated in a study with phase imaging, sensitive to paramagnetic tissue.[6] Voxel-based morphometry (VBM) and diffusion tensor imaging (DTI) studies of the brain showed cortical gray and white matter changes, e.g., in the sensorimotor cortex[7,8] and frontal/parietal areas,[9] and other central structures such as the thalamus,[10] basal ganglia, hypothalamus, substantia nigra, red nucleus, cerebellum, and inferior olive.[11,12] However, the findings differed substantially between studies.[11] Applications based on nuclear medicine techniques showed partly conflicting results in the basal ganglia, whereas one study demonstrated an altered D2-receptor binding potential also in extrastriatal brain areas.[13]

It might be assumed that RLS reflects a disturbance in various functional systems of the central nervous system and that the integration of these functional systems may be most relevant for the understanding of RLS.[12] Both clinical presentation (i.e., a "spinal" pattern of the distribution of the symptoms, i.e., classically involving both lower limbs in a fairly symmetrical pattern) and technical studies suggest that spinal alterations might have a substantial role in the pathophysiology of RLS.[3,14,15] In connection with the involvement of dopamine the spinal cord might be assigned an important role together with the involved brain areas.[16,17]

Despite the putative involvement of the spinal cord in the pathophysiology of RLS, there is no imaging study yet that specifically addresses the brainstem and the spinal cord by computer-based MRI in idiopathic RLS. DTI is a quantitative MRI-based analysis technique of white matter (WM) integrity that provides information about the microstructural properties of tissue[18] and seems to be the optimal technical candidate for this purpose. Thus, the aim of this study was to use DTI in spinal diffusion-weighted MRI data of patients with idiopathic RLS in order to analyze and quantify WM tract integrity in the cervical spinal cord up into the brainstem until the midbrain.

METHODS

Subjects and Clinical Characterization

Twenty-five patients (17 female and 8 male; mean age ± standard deviation (SD), 63.2 ± 10.3 y) with idiopathic RLS and

25 healthy controls (16 female and 9 male; mean age ± SD, 60.2 ± 12.4 y) were included in the study. Patients were recruited from the Outpatient Clinic of the Department of Neurology, University of Ulm, Germany, whereas healthy controls were recruited from interested volunteer groups of the University of Ulm and from the relatives of the patients. The protocol was approved by the Ethics Committee of the University of Ulm, Germany, and written informed consent was obtained from all patients and controls before inclusion.

All patients fulfilled the revised essential criteria for the diagnosis of idiopathic RLS defined by the International RLS Study Group (IRLSSG).[2] Since 2011, the IRLSSG revised essential diagnostic criteria include a fifth point allowing a diagnosis of RLS solely if the typical RLS symptoms are not accounted for by symptoms in the context of other medical or behavioral conditions (http://irlssg.org/). The duration of RLS symptoms was 11.6 ± 9.5 y (range 2–40 y). The international RLS severity scale (IRLS) assessing symptom severity of the 7 d before the MRI measurements indicated severe RLS symptoms with a mean score of 27 ± 9 points. None of the patients had any features of symptomatic RLS on the basis of clinico-neurological examination, electroneurography, and laboratory studies (including serum ferritin levels). All but two patients (who were medication free) were on dopaminergic medication in usual dosages (levodopa, n = 9; pramipexole, n = 11; rotigotine, n = 2; ropinirole, n = 1); none of the patients was treated with any other substance classes such as opioids. All patients were asked to stop taking the RLS medication 24 h before the MRI examination. However, seven patients, due to intolerable symptoms, took their medication on the day of the MRI acquisition but with a time interval of at least 6 h before the MRI.

The control sample had no history of any clinically relevant neurological or psychiatric disease or other medical conditions. Specifically, any brain pathology including microvascular brain alterations was excluded by conventional MRI.

The MRI investigations took place during the evening hours (between 19:00 and 21:00) at a time when RLS patients usually have symptoms. During the investigation of approximately 40 min, the severity of sensory symptoms was assessed according to the SIT protocol (Suggested Immobilization Test[19]).

MRI Acquisition

The scanning protocols were performed on a 1.5 Tesla Magnetom Symphony (Siemens Medical, Erlangen, Germany). The DTI study protocol of the brainstem was identical for patients with RLS and controls and consisted of 31 volumes (56 slices, 128 × 128 pixels, slice thickness 2.5 mm, pixel size 2.5 × 2.5 mm^2), representing 30 gradient directions and one scan with gradient 0 (b = 0). The echo time (TE) and repetition time (TR) were 102 ms and 8,000 ms, respectively; b was 800 s/mm^2 and two scans were averaged online by the scanner software in image space.

The DTI study protocol of the cervical spinal cord covered the area from apex dentis to the seventh vertebra and was also identical for patients with RLS and controls. It consisted of 13 volumes (55 slices, 128 × 124 pixels, slice thickness 2.0 mm, pixel size 2.0 × 2.0 mm^2), representing 12 gradient directions and one scan with gradient 0 (b = 0). TE and TR were 96 ms and 11,900 ms, respectively; b was 800 s/mm^2 and four scans were averaged in image space. For the anatomical z-range estimation, a T1-weighted spin-echo was recorded for each patient and control subject (TR 550 ms, TE 11 ms, matrix size 384 × 384 pixels, 10 slices, voxel size 0.65 × 0.65 × 3.00 mm^3). Only the cervical spinal cord was scanned because of technical reasons and restrictions of time due to the patients` limited tolerance to immobilization.

As the quality assessment for movement artefacts, an outlier-based method was used that had been specifically developed to identify movement and other sources of noise by comparing the index DWI direction against a weighted average computed from all other directions of the same subject.[20]

Data Analysis: Postprocessing of Brainstem Data

The DTI analysis software Tensor Imaging and Fibre Tracking (TIFT)[21] was used for all postprocessing and statistical analysis. All DTI data sets of the brain were spatially normalized on the Montreal Neurological Institute (MNI) stereotactic standard space; the entire normalization process has already been described elsewhere.[22] After the normalization procedure, all individual DTI datasets were used for the calculation of the second-rank diffusion tensor and the fractional anisotropy (FA) for quantification of the diffusion anisotropy, according to standard methods.[18] For smoothing, an 8-mm full width at half maximum gaussian filter was applied within the whole brain-based statistics (WBSS) in order to achieve a good balance between sensitivity and specificity.[23] The analysis volume was restricted to the caudal parts of the brain from the medulla oblongata until the midbrain.

Statistical comparison between the RLS group and the control group was performed voxelwise by Student *t* test, i.e., FA values of the patients' FA maps were compared with the FA values of the controls' FA maps for each voxel separately. FA values below 0.2 were not considered for calculation (cortical gray matter shows FA values up to 0.2[24]). Statistical results were corrected for multiple comparisons at the voxel level using the false-discovery-rate (FDR) algorithm at $P < 0.05$.[25] Further reduction of the alpha error was performed at the cluster level by a spatial correlation algorithm that eliminated isolated voxels or small isolated groups of voxels in the size range of the acquisition voxel size, leading to a lean threshold cluster size of 300 voxels (300 mm^3)—this cluster size threshold was used by keeping the relation of cluster size threshold and acquisition voxel size constant.[8]

Data Analysis: Postprocessing of Spinal Cord Data

For spatial normalization, fixation points along the spinal cord were determined. As a global reference point, apex dentis was identified by an experienced operator in each data set. Spinal cord axial slices were normalized by linearization of the spinal cord (Figure 1A and 1C). Axial stretching reference was determined from morphological sagittal slices (Figure 1B), thus normalizing all datasets to the distance between apex dentis and the seventh cervical vertebra. A spinal cord mask was created from a template that was obtained by arithmetically averaging b = 0 images of all subjects (Figure 1D). After filtering with a full width at half maximum of 8 mm, averaged FA

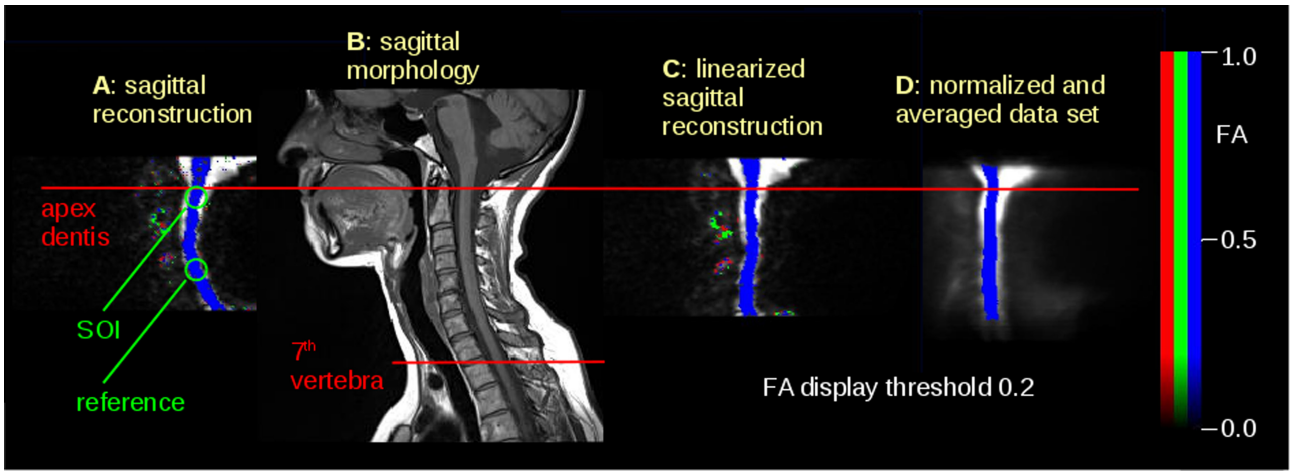

Figure 1—Illustration of the normalization process. **(A)** Sagittal reconstruction of axial DTI scans – FA map (blue = apical-basal), crosshairs at apex dentis. Background is the (b = 0)-scan. **(B)** Sagittal morphological T1w scan to calculate the distance between apex dentis and seventh vertebra, as indicated by lines. **(C)** Axially normalized FA map of (A). **(D)** Template obtained from axially normalized FA maps; slices of interest (SOIs) are indicated by horizontal lines. DTI, diffusion tensor imaging; FA, fractional anisotrophy.

Table 1—Clusters of voxelwise comparison of fractional anisotropy at the group level.

Cluster	MNI (x / y / z)	Hemisphere	Cluster Size	Level of Significance (FDR Corrected)	Anatomical Localization
1	9 / −31 / −14	Right	723	< 0.00001	Midbrain
2	−8 / −18 / −7	Left	305	0.00002	Midbrain

Clusters of whole brain-based spatial statistics at P < 0.05, FDR corrected, comparison of fractional anisotropy maps of patients with restless legs syndrome and controls. FDR, false discovery rate; MNI, Montreal Neurological Institute.

values for each slice for each subject were calculated within the mask region for FA values greater than 0.2 because FA values less than 0.2 were defined as outside the spinal cord according to previous studies.[26]

Data analysis was performed in a twofold manner: First, a hypothesis-driven approach was performed, placing slices of interest (SOIs) at the level of the first cervical vertebra area as well as at the level of the third vertebra area, which were manually determined by an experienced operator (JK; Figure 1A). Group comparison was performed for the relative averaged FA values within a region of interest of r = 10 mm in this region, i.e., the ratio of SOI values to reference values. This approach ensured that the normalization process did not bias the output results of the FA comparison of stereotaxically normalized datasets.

Second, a hypothesis-free approach was applied by slicewise averaging of FA values of the spinal cord (five subsequent slices of 1-mm thickness), and statistical comparison between patients with RLS and controls at the group level was done. Pearson correlation to disease duration and IRLS, respectively, was performed for each of the normalized FA slices.

RESULTS

Clinical Data

Patients reported a strong urge to move during the MRI acquisition, but no patient stopped the investigation. According to SIT data, patients showed an increase of symptom severity from a mean of 1 (maximum, 10) at the beginning of the MRI measurement up to 4 ± 3 at the end, whereas controls were stable at 0 ± 1. The specifically dedicated quality assessment for movement artefacts was applied to the MRI data in order to discover noise according to movement[20] and did not discover disturbed acquisition volumes in any of the data sets.

Midbrain/Brainstem Analysis

Voxelwise statistical comparison of FA maps in the brainstem revealed significant differences between patients and healthy controls at P < 0.05 after FDR correction. The alterations were localized in two clusters in the midbrain, one was left-sided and one was right-sided (Table 1, Figure 2). Individual averaged FA values within the clusters did not significantly correlate to disease duration or IRLS.

Spinal Cord Analysis

Slicewise FA values were analyzed in the SOI in a hypothesis-guided approach. Here, averaged FA values in the SOI were normalized to the average FA value of controls in the corresponding position, thus obtaining relative FA values. The group comparison of relative FA values of SOIs at the level of the first vertebra area demonstrated group differences at uncorrected P < 0.05 (Figure 3A).

Slicewise FA analysis showed similar curve patterns along the spinal cord for patients and controls. There were different

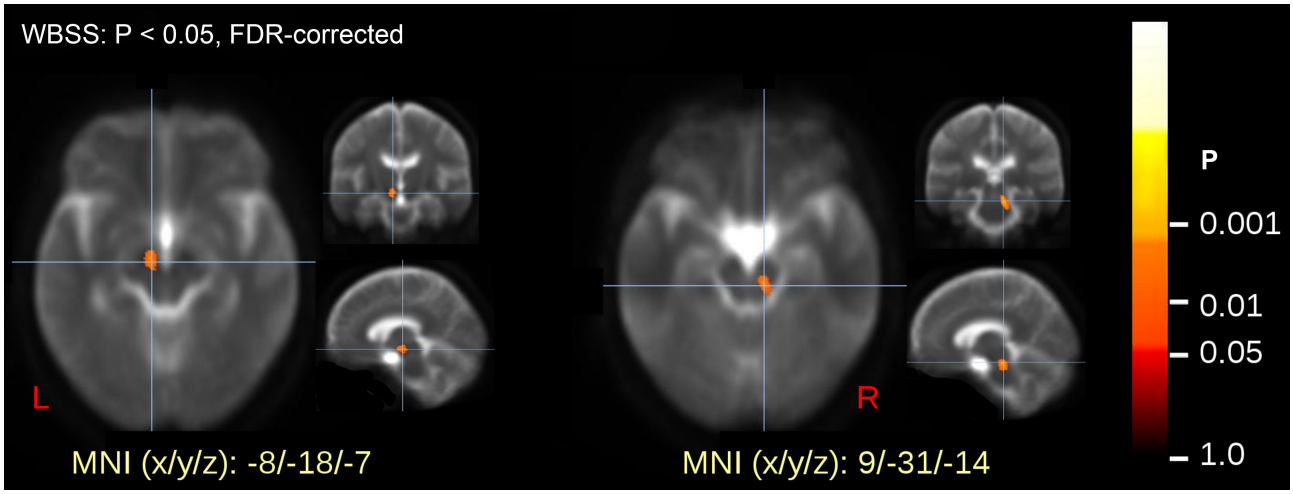

Figure 2—Voxelwise comparison of fractional anisotrophy (FA) maps (whole brain-based spatial statistics [WBSS]) of patients and controls with significance level at P < 0.05. Values are false discovery rate (FDR)-corrected and revealed two significant clusters in the midbrain bilaterally.

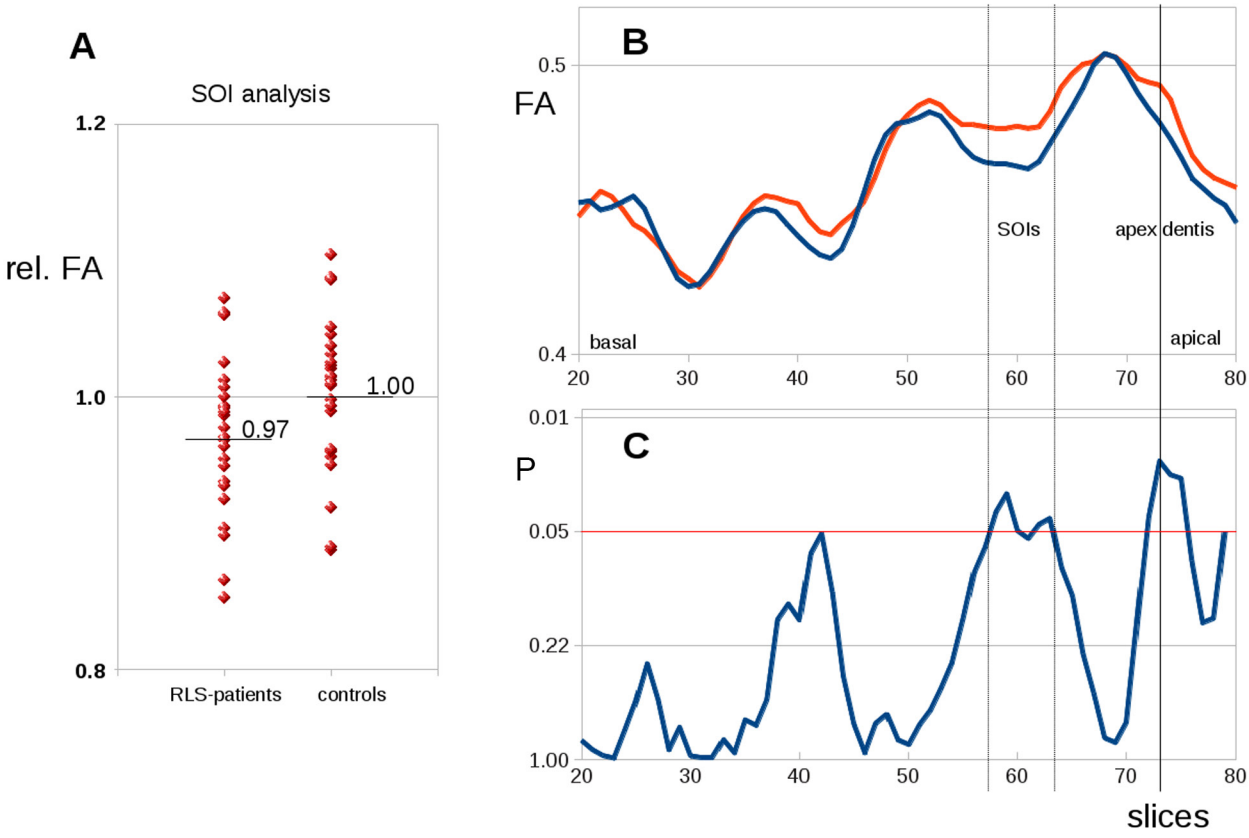

Figure 3—**(A)** Group differences between patients with restless legs syndrome (RLS) and controls of fractional anisotrophy (FA) values in operator-defined slices of interest (SOI) within the spinal cord. **(B)** Group averaged slicewise FA values along the cervical spinal cord for patients with RLS (red) and controls (blue). **(C)** Differences along the cervical spinal cord (T test values, significance level P < 0.05, uncorrected).

FA values between patients with RLS and controls at the level of the first, second, and third vertebra area at uncorrected P < 0.05 (dashed lines in Figure 3B and 3C). Slices where slicewise FA values showed differences of P < 0.05 (at the level of the first, second, and third vertebra area) were defined as SOI in the subsequent analysis—the SOI placement was identical to the predefined operator-based SOI localization. Slicewise FA values were correlated with disease duration (Pearson correlation), and a correlation with P < 0.05 was found in the SOI.

However, no significance for either slicewise FA values and for correlation with disease duration was found when the results for the series of slices were corrected for multiple comparisons (Bonferroni-Holm procedure), because none of the results found survived this correction.

DISCUSSION

In this study, significant alterations of microstructure were observed in the midbrain bilaterally by unbiased voxelwise comparison of patients with RLS with healthy controls at corrected $P < 0.05$. In addition, DTI-based analysis of the cervical cord demonstrated reduced regional FA at the level of the second and third vertebra in patients with RLS versus controls at uncorrected $P < 0.05$; however, these results did not survive corrections for multiple comparisons.

Significantly altered microstructure of the midbrain in patients with RLS was demonstrated by DTI for the first time, to the best of our knowledge. The clusters were located bilaterally, on the left side extending into the area of the substantia nigra, on the right side in close proximity to it, i.e., a structure considered to be involved in current theories of the pathophysiology of primary RLS.[27] In general concordance with our data, previous investigations by use of transcranial sonography described abnormal findings in this area, including hypoechogenicity of the substantia nigra and raphe as well as hyperechogenicity of the red nucleus.[28]

This hypothesis guided study assesed midbrain/brainstem and spinal cord involvement in RLS by MRI, because the clinical pattern of RLS (i.e., classically symmetrical involvement of lower limbs) suggests this pathology. Also with respect to theoretical concepts of RLS, these areas are to be involved because the dopaminergic A11 neurons that spread to the midbrain/brainstem and lead to spinal pathways are consistently assumed to be part of the RLS etiology.[12] Specifically, A11 clusters are known to be located in the brainstem up to the midbrain.[3] The (existing) further projections into the cortex and the limbic system were not addressed in this study because too many white matter pathways are located here and may mask specific alterations. The results of the study with significant findings in the midbrain in areas with A11 clusters are in concordance with the proposed association of the observed fiber tract alterations (FA reductions) with the A11 cell group. The midbrain is in close proximity to the A11 cell group in the hypothalamus, which is the primary source of descending dopaminergic input into the spinal cord. However, morphological damage to the A11 cell areas has not been demonstrated in postmortem data, because a controlled autopsy study of the hypothalamic A11 cell bodies in six RLS cases demonstrated no significant difference between RLS or control cases on any measure used.[29]

For a given unbiased analysis of the spinal cord, the results both for FA value comparison between patients and controls and for correlations between disease duration and FA have to be considered negative, thus indicating no involvement of the diffusion-related properties of the spinal cord in RLS. In contrast, an operator-driven approach that defined the SOI at the level of the second and third vertebra resulted in significant differences in diffusion metrics. This constellation demonstrates the ambivalence between the hypothesis-free approach and the operator-guided approach defining well-selected regions to be analyzed. The current results at the uncorrected level cannot provide a final statement, but a trend of differences of diffusion metrics within the spinal cord can be held so that further studies, e.g., at higher magnetic field strengths, might readdress this question. This study suggests that, beyond the alterations in the midbrain, an involvement of the spinal cord in RLS can be visualized by DTI and that an area of interest is regionally clustered in the upper cervical spinal cord.

FA could provide a meaningful microstructural metric, as a confirmation of the hypothesis that DTI as a technique that addresses WM structures and tracts was the best technical approach to the aims of the study. Neuropathological studies report a decrease in myelin in the brains of individuals with RLS, i.e., there is evidence of less myelin and loss of myelin integrity in RLS brains coupled with decreased ferritin and transferrin in the myelin fractions.[30] DTI seems to be the best candidate for the transfer of these findings to *in vivo* neuroimaging due to its capacities to image WM microstructure. With respect to the spinal cord study, the methodological approach used here carried forward a previous DTI study[26] by the use of axial slices instead of coronal slices and that spatial normalization was controlled for by manual positioning of SOIs using the information of the whole spinal cord analysis as a reference.

Our study has several limitations. First, the DTI findings as they stand comprise a microstructural reduction in directionality of the fiber tracts in this position that cannot be further differentiated with respect to its nature. Second, the results at the spinal cord level did not survive corrections for multiple comparisons so that only a tendency toward RLS-associated altered diffusion metrics within the spinal cord might be stated, which needs to be addressed further. Third, one shortcoming of the technical approach to the spinal cord was that it did not allow differentiation between subareas such as the ventral or dorsal horn, and also that only a magnetic field strength of 1.5 Tesla was used, thus limiting spatial resolution. This differentiation also has to await future studies with a more subtle approach to spinal cord substructure, most probably at higher field strengths.

In summary, with respect to the refinement of RLS pathoanatomy, the regional FA reduction in the midbrain might correlate with a macroscopically subtle process with changes of the tissue microstructure in the corresponding tracts. It still remains to be seen if the functional pathways were either altered primarily as a causative pathophysiological correlate of RLS or if the abnormalities result as a correlate of central nervous system plasticity in the course of the disorder.[8] Understanding the full range of RLS-associated neuropathology is an important aim because it may help us improve our approach to the complex nature of its clinical features and expand our considerations of treatment options.

REFERENCES

1. Berger K, Kurth T. RLS epidemiology - frequencies, risk factors and methods in population studies. Mov Disord 2007;18:S420–3.

2. Allen RP, Picchietti D, Hening WA, Trenkwalder C, Walters AS, Montplaisir J. Restless legs syndrome: diagnostic criteria, special considerations and epidemiology. A report from the restless legs syndrome diagnosis and epidemiology workshop at the National Institutes of Health. Sleep Med 2003;4:101–19.
3. Trenkwalder C, Paulus W, Walters AS. The restless legs syndrome. Lancet Neurol 2005;4:465–75.
4. Ondo WG, He Y, Rajasekaran S, Le WD. Clinical correlates of 6-hydroxydopamine injections into A11 dopaminergic neurons in rats: a possible model for restless legs syndrome. Mov Disord 2000;15:154–8.
5. Allen RP, Barker PB, Wehrl F, Song HK, Earley CJ. MRI measurement of brain iron in patients with restless legs syndrome. Neurology 2001;56:263–5.
6. Rizzo G, Manners D, Testa C, et al. Low brain iron content in idiopathic restless legs syndrome patients detected by phase imaging. Mov Disord 2013;28:1886–90.
7. Unrath A, Juengling FD, Schork M, Kassubek J. Cortical grey matter alterations in idiopathic restless legs syndrome: an optimized voxel-based morphometry study. Mov Disord 2007;22:1751–6.
8. Unrath A, Müller HP, Ludolph AC, Riecker A, Kassubek J. Cerebral white matter alterations in idiopathic restless legs syndrome, as measured by diffusion tensor imaging. Mov Disord 2008;23:1250–5.
9. Chang Y, Chang HW, Song H, et al. Gray matter alteration in patients with restless legs syndrome: a voxel-based morphometry study. Clin Imaging 2015;39:20–5.
10. Etgen T, Draganski B, Ilg C, et al. Bilateral thalamic gray matter changes in patients with restless legs syndrome. Neuroimage 2005;24:1242–7.
11. Rizzo G, Tonon C, Manners D, Testa C, Lodi R. Imaging brain functional and metabolic changes in restless legs syndrome. Curr Neurol Neurosci Rep 2013;13:372.
12. Trenkwalder C, Paulus W. Restless legs syndrome: pathophysiology, clinical presentation and management. Nat Rev Neurol 2010;6:337–46.
13. Cervenka S, Pålhagen SE, Comley RA, et al. Support for dopaminergic hypoactivity in restless legs syndrome: a PET study on D2-receptor binding. Brain 2006;129:2017–28.
14. Telles SC, Alves RC, Chadi G. Periodic limb movements during sleep and restless legs syndrome in patients with ASIA A spinal cord injury. J Neurol Sci 2011;303:119–23.
15. Bachmann CG, Rolke R, Scheidt U, et al. Thermal hypoaesthesia differentiates secondary restless legs syndrome associated with small fibre neuropathy from primary restless legs syndrome. Brain 2010;133:762–70.
16. Paulus W, Schomburg ED. Dopamine and the spinal cord in restless legs syndrome: does spinal cord physiology reveal a basis for augmentation? Sleep Med Rev 2006;10:185–96.
17. Trenkwalder C, Paulus W, Walters AS. The restless legs syndrome. Lancet Neurol 2005;4:465–75.
18. Basser PJ, Jones DK. Diffusion-tensor MRI: theory, experimental design and data analysis - a technical review. NMR Biomed 2002;15:456–67.
19. Montplaisir J, Boucher S, Poirier G, Lavigne G, Lapierre O, Lespérance P. Clinical, polysomnographic, and genetic characteristics of restless legs syndrome: a study of 133 patients diagnosed with new standard criteria. Mov Disord 1997;12:61–5.
20. Müller HP, Süssmuth SD, Landwehrmeyer GB, et al. Stability effects on results of diffusion tensor imaging analysis by reduction of the number of gradient directions due to motion artifacts: an application to presymptomatic Huntington's disease. PLoS Curr 2011;3:RRN1292.
21. Müller HP, Unrath A, Ludolph AC, Kassubek J. Preservation of diffusion tensor properties during spatial normalization by use of tensor imaging and fibre tracking on a normal brain database. Phys Med Biol 2007;52:N99–109.
22. Müller HP, Kassubek J. Diffusion tensor magnetic resonance imaging in the analysis of neurodegenerative diseases. J Vis Exp 2013;(77):e50427. doi: 10.3791/50427.
23. Unrath A, Mueller HP, Riecker A, Ludolph AC, Sperfeld AD, Kassubek J. Whole brain-based analysis of regional white matter tract alterations in rare motor neuron diseases by diffusion tensor imaging. Hum Brain Mapp 2010;31:1727–40.
24. Kunimatsu A, Aoki S, Masutani Y, et al. The optimal trackability threshold of fractional anisotropy for diffusion tensor tractography of the corticospinal tract. Magn Reson Med Sci 2004;3:11–7.
25. Genovese CR, Lazar NA, Nichols T. Thresholding of statistical maps in functional neuroimaging using the false discovery rate. Neuroimage 2002;15:870–8.
26. Nair G, Carew JD, Usher S, Lu D, Hu XP, Benatar M. Diffusion tensor imaging reveals regional differences in the cervical spinal cord in amyotrophic lateral sclerosis. Neuroimage 2010;53:576–83.
27. Dauvilliers Y, Winkelmann J. Restless legs syndrome: update on pathogenesis. Curr Opin Pulm Med 2013;19:594–600.
28. Godau J, Sojer M. Transcranial sonography in restless legs syndrome. Int Rev Neurobiol 2010;90:199–215.
29. Earley CJ, Allen RP, Connor JR, Ferrucci L, Troncoso J. The dopaminergic neurons of the A11 system in RLS autopsy brains appear normal. Sleep Med 2009;10:1155–7.
30. Connor JR, Ponnuru P, Lee BY, et al. Postmortem and imaging based analyses reveal CNS decreased myelination in restless legs syndrome. Sleep Med 2011;12:614–9.

SUBMISSION & CORRESPONDENCE INFORMATION

Submitted for publication April, 2015
Submitted in final revised form September, 2015
Accepted for publication September, 2015
Address correspondence to: Professor Jan Kassubek, MD, Department of Neurology, University of Ulm, Oberer Eselsberg 45, 89081 Ulm, Germany; Tel: + 49 731 1771206; Fax: + 49 731 1771202; Email: jan.kassubek@uni-ulm.de

DISCLOSURE STATEMENT

This was not an industry supported study. The authors have indicated no financial conflicts of interest. There was no investigational or off-label use.